

First Clinical Experience of Tungsten Rubber Electron Adaptive Therapy With Real-time Variable-shape Tungsten Rubber

YOSHIHIRO KAWAI¹, MIKOTO TAMURA², MORIKAZU AMANO¹, TAKASHI KOSUGI³ and HAJIME MONZEN²

¹Department of Radiology, Fujieda Municipal General Hospital, Shizuoka, Japan;

²Department of Medical Physics, Graduate School of Medical Sciences, Kindai University, Osaka, Japan;

³Department of Radiation Oncology, Fujieda Municipal General Hospital, Shizuoka, Japan

Abstract. *Background/Aim:* We investigated the dosimetric characteristics of electron radiotherapy for auricular keloid using real-time variable-shape tungsten rubber (STR). *Patients and Methods:* For the first evaluation, STR was shaped into a rectangular irradiation field ($3.0 \times 5.0 \text{ cm}^2$). In the next step, the STR was reshaped to fit the target ($3.5 \times 6.5 \text{ cm}^2$) for the second evaluation. Percentage depth doses (PDDs) and lateral dose profiles were obtained with 6-MeV electron beams and compared with those of low-melting-point lead (LML). *Results:* Compared to the LML on electron applicator, PDD differences were within 0.4 mm, while the penumbras as width of 20-80% dose levels were smaller (maximum reductions: 75.8% and 82.9% at first and second evaluations, respectively). The treatment process of shaping the STR, decision on output, and irradiation was completed within 45 min. *Conclusion:* Electron radiotherapy using STR for keloid can be performed with excellent dose distribution in a short time. First clinical experience found the STR is suitable for use in individualized and immediate electron radiotherapy.

Low-melting-point lead (LML) is generally used to shape the irradiation field in megavoltage electron radiotherapy (1-4). However, it is associated with several problems, such as the fact that shaping the collimator of the irradiation field is time-consuming and its toxicity to the human body and the environment (5-8). Additionally, the air gap between the LML on an electron applicator and the patient causes a large penumbra (9, 10), requiring a large margin in clinical delivery.

Correspondence to: Hajime Monzen, Ph.D., Department of Medical Physics, Graduate School of Medical Sciences, Kindai University, 377-2 Onohigashi, Osakasayama, Osaka, 589-8511, Japan. E-mail: hmon@med.kindai.ac.jp

Key Words: Real-time variable-shape tungsten rubber, electron radiotherapy, keloid scar, tungsten rubber electron adaptive therapy (TREAT).

We have reported some radiation-shielding materials made of tungsten such as tungsten functional paper (TFP) (11-18) and tungsten-containing rubber (TCR) (8, 19-21) and their applications to clinical sites. Recently, we have newly developed a real-time variable-shape tungsten rubber (STR) (Hayakawa Rubber Co., Ltd. Hiroshima, Japan) (22). The STR has several advantages over TFP and TCR, such as being easy to shape by hand at approximately 60°C and the shape can be maintained at room or body temperatures. It has adequate radiation-shielding ability against megavoltage electron beams and γ -rays for brachytherapy (22). Therefore, STR is anticipated to be employed at clinical sites instead of LML and lead (23, 24).

In clinical practice, patients who develop a keloid on their earlobe or abdomen should undergo electron radiotherapy as soon as possible after excision because the recurrence rate of keloid scars was shown to be reduced when radiation was applied within 7 hours as compared to 24 hours or longer after excision (25). Performing conventional electron radiotherapy with LML is exceedingly difficult immediately after excision. Additionally, LML cannot adapt to the movements of the target in terms of respiration and patient motion. In contrast, all these problems can be resolved with STR (22).

In this study, STR was used for skin field collimation in postoperative electron radiotherapy of auricular keloid in actual clinical delivery for the first time worldwide. This novel method was named tungsten rubber electron adaptive therapy (TREAT). We aimed to introduce the process of utilizing STR in the clinical setting and summarize its advantages in clinical and dosimetric approaches.

Patients and Methods

STR characteristics. STR is a rubbery material with no cross-linked polymerization and is a real-time variably shaped material. Its density is 7.3 g/cm^3 . The elemental ratio (wt%) in STR is C: 5.5%, H: 0.9%, O: 1.4%, and W: 92.2%. Physical characteristics of STR are well explained in a previous report (22).

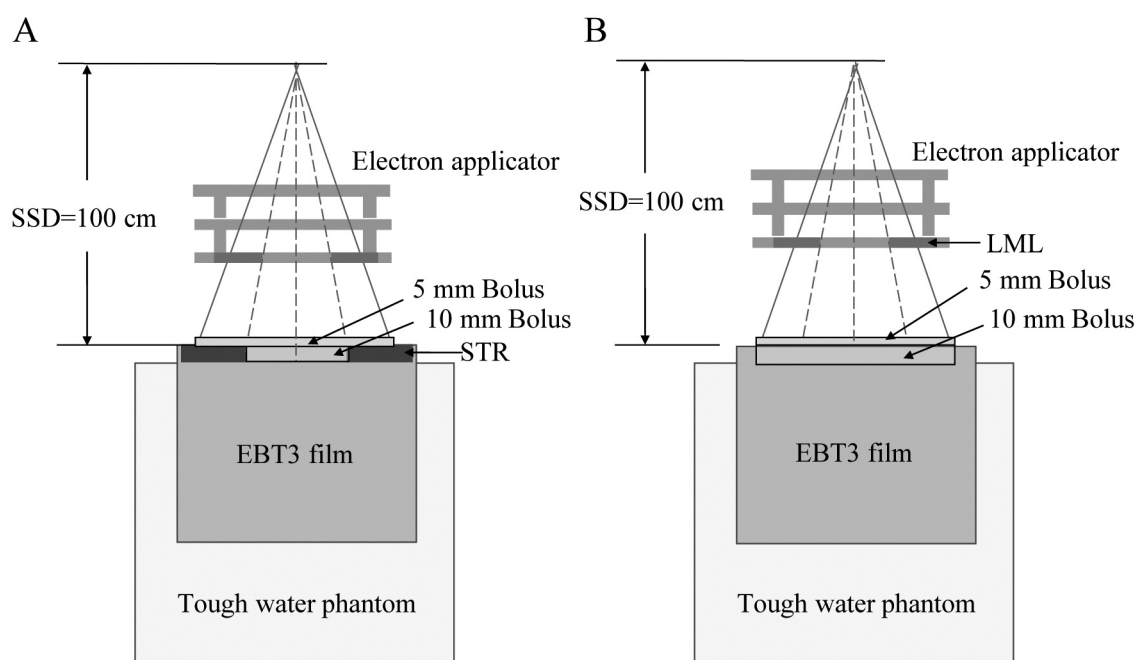


Figure 1. Experimental setup for the measurement of the 2D dose distributions for variable-shape tungsten rubber (STR) (A) and low-melting-point lead (LML) (B).

Patient characteristics. The patient (female, 32 y.o.) investigated in this study had keloid recurrence and underwent repeat excision for right auricular keloid due to earring scars. A large keloid of $2.0 \times 1.5 \times 1.0 \text{ cm}^3$ recurred at the right helix of the auricle, and electron radiotherapy was required for its curative treatment because she had not undergone radiotherapy at that site. Informed consent from this patient was obtained, and this study was approved by the Ethics Committee (Approval No. 2020-009) at Fujieda Municipal General Hospital. All procedures were carried out in accordance with the Declaration of Helsinki.

STR shaping and setup. Firstly, wrapped in clingfilm the STR was heated at 700 W for 1 min in a microwave oven, and then shaped into a rectangular form, which was denoted as basic STR. The electron beam energy was set at 6 MeV (25-28) from a clinical linear accelerator (linac) (Infinity; Elekta AB, Stockholm, Sweden), and the irradiation field was $3.0 \times 5.0 \text{ cm}^2$ at a source-to-surface distance (SSD) of 100 cm. The STR thickness was 10 mm to provide adequate shielding of the 6 MeV electron beam (22). The square electron applicator (field size: $10 \times 10 \text{ cm}^2$ at SSD of 100 cm) was set, and LML collimation with a circular shape of 6 cm in diameter at SSD of 100 cm was set on the applicator. This process was completed within only 15 min.

Dosimetric evaluation prior to electron radiotherapy. We performed dosimetric evaluation prior to electron radiotherapy. The STR was set on a water-equivalent phantom (Tough Water Phantom, WD3005; Kyoto Kagaku, Kyoto, Japan), and the two-dimensional (2D) dose distribution was measured with EBT3 Gafchromic™ film (Ashland, KY, USA). The distance from the source to the surface of the STR was 100 cm to simulate clinical delivery. A bolus with

10 mm thickness was placed in the aperture for the irradiation field with the STR to simulate the auricle. The film was set up parallel to the central beam axis (CAX). The film analysis was performed using a scanner (ES-G11000; Epson, Nagano, Japan) and software (DD-Analysis system version 10.55; R-TECH, Tokyo, Japan) at least 24 h after irradiation (29) with a resolution of 72 dpi from the red channel. The linac output in monitor units was 200 MU, and the percentage depth doses (PDDs) and lateral dose profiles on the long axis of the STR were obtained from the 2D dose distributions. The lateral dose profiles were normalized to the dose at CAX. A conventional LML collimator with the same irradiation field size at SSD of 100 cm was also employed, and the PDD and lateral dose profile were obtained using the same measurement method in order to compare the dosimetric characteristics between the novel irradiation method with the STR and conventional irradiation method with the LML. The LML thickness was 1.6 cm. Figure 1 shows the experimental geometries for the STR and LML collimators. The PDD characteristics were evaluated based on the depths of maximum dose (d_{max}), 90% dose (d_{90}), 80% dose (d_{80}), and 50% dose (d_{50}). Then the penumbral width (defined as the width of the off-axis distance from 80% to 20% dose levels, P_{80-20}) was obtained from these lateral dose profiles at d_{max} , d_{90} , d_{80} , and under the STR (d_{15mm}), and the reduction rate was evaluated using the following equation:

$$\text{Reduction rate} = \frac{(P_{LML} - P_{STR})}{P_{LML}} \times 100 (\%) \quad (\text{Equation 1})$$

where P_{LML} and P_{STR} were the penumbral widths (P_{80-20}) using the STR and LML, respectively.

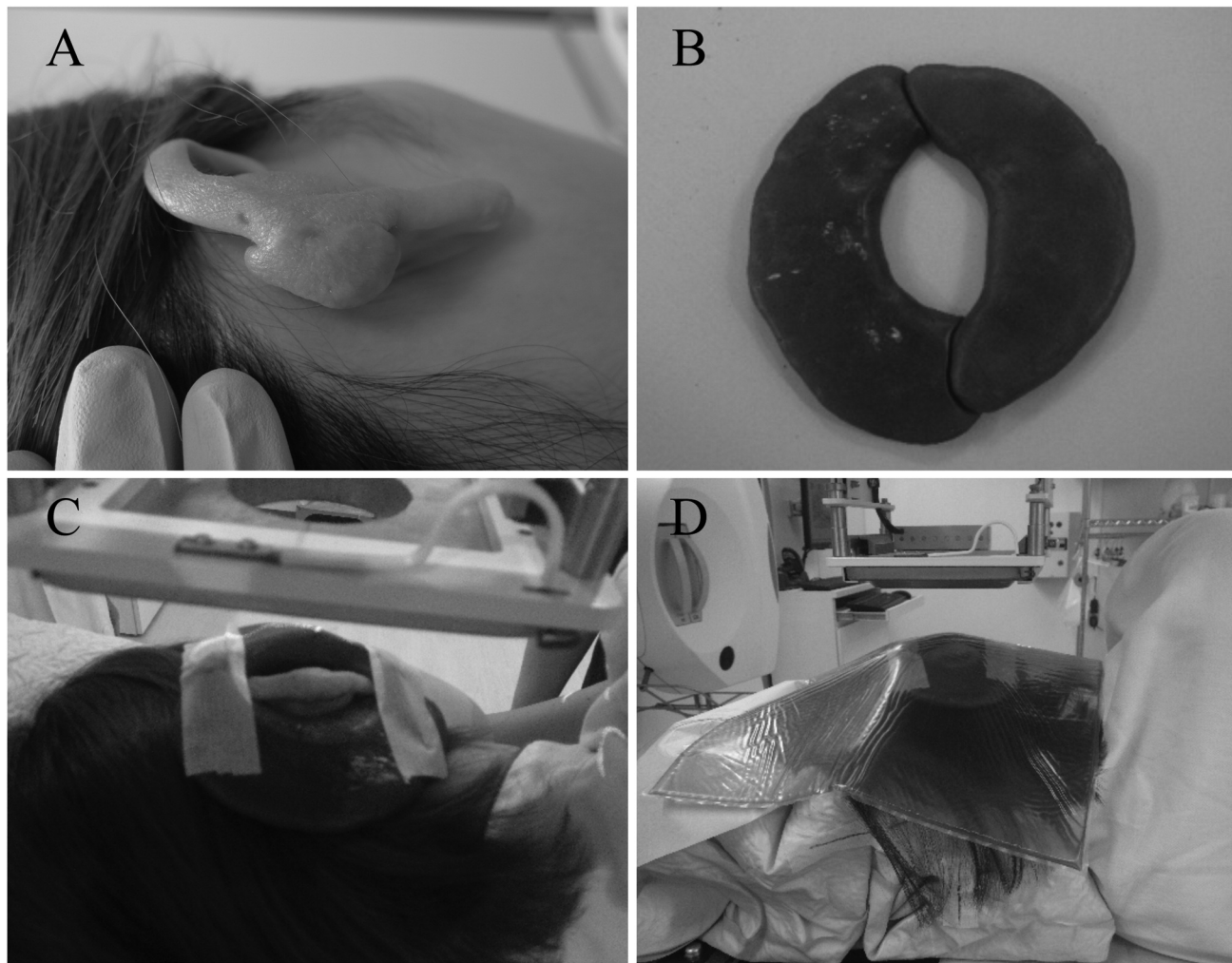


Figure 2. A: Keloid scar on the cartilage of the right ear. B: Variable-shape tungsten rubber shaped for therapy delivery (clinical STR). C: Actual setup for therapy. D: Delivery of electron radiotherapy with 5 mm bolus.

Clinical delivery. The STR, wrapped in clingfilm, was heated at 700 W for 1 min using a microwave. The STR was then shaped on the desk roughly and reshaped by hand to cover the whole auricle adaptively, denoted as clinical STR, with the patient on the treatment couch and her head immobilized. Figure 2 shows the clinical delivery images. The keloid, which recurred at the right helix of the auricle, is shown in Figure 2A. The aperture size for irradiation was approximately $3.5 \times 6.5 \text{ cm}^2$ (Figure 2B). The auricle of the patient was inserted into the clinical STR, and the two parts of the STR were combined and held in place with tape as shown in Figure 2C. Additionally, a bolus with 5 mm thickness was set on the surface of the STR (Figure 2D). With the patient off the treatment couch, we evaluated the output factor for the actual irradiation field with a parallel plate ionization chamber (Advanced Markus Ion Chamber; PTW, Freiburg, Germany) at d_{max} in the Tough Water Phantom. The output factor is the ratio of the dose for a given field size to the dose for the reference field size (*e.g.*

$10.0 \times 10.0 \text{ cm}^2$). This factor increases with increasing field size due to scatter radiation. The prescribed dose was 10 Gy/2 fr. Finally, the irradiation number of MU was decided by using the output factor to deliver the prescribed dose of 5 Gy/fr, and the clinical delivery was performed.

Dosimetric evaluation after electron radiotherapy. The second dosimetric evaluation was performed for the clinical irradiation field after the delivery. The LML was also shaped in accordance with the shape of the clinical STR to compare the dosimetric characteristics. The experimental setup was similar to that of the dosimetric evaluation before the electron radiotherapy as shown in Figure 1. The 2D dose distribution was obtained using the film set up parallel to the CAX. Lateral dose profiles at d_{max} , d_{90} , and d_{80} and $d_{15\text{mm}}$ in the preoperative evaluation were obtained. Then the penumbral widths were also obtained from those lateral dose profiles, and the reduction rates were evaluated using Equation 1.

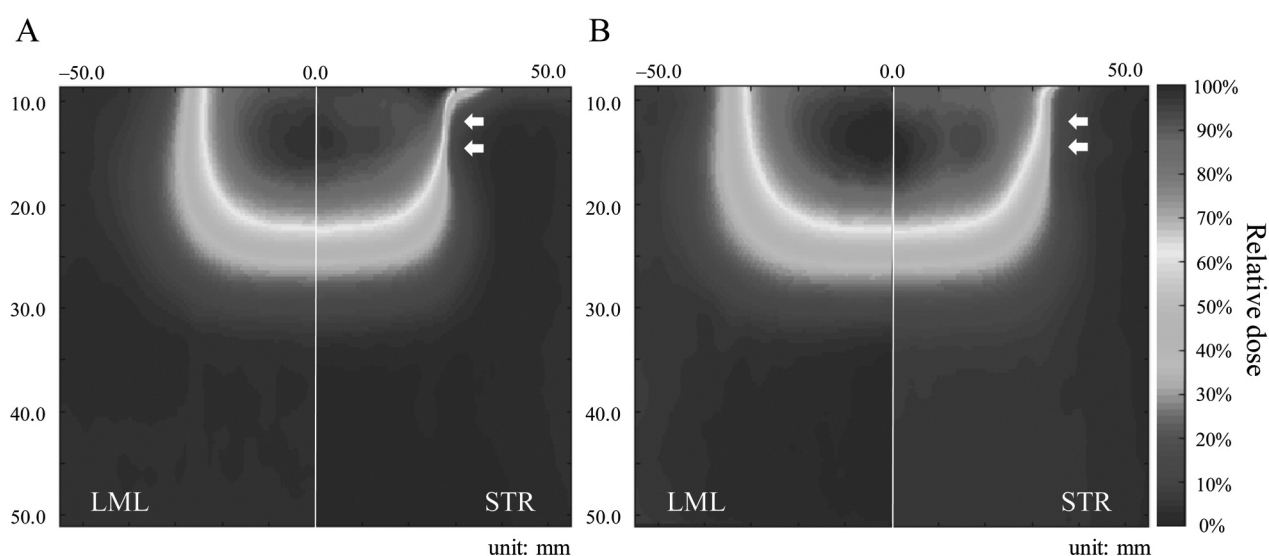


Figure 3. Two-dimensional dose distributions for first (A) and second (B) dosimetric evaluation using basic and clinical variable-shape tungsten rubber (STR), respectively. White arrows indicate the sharp penumbra with the STR.

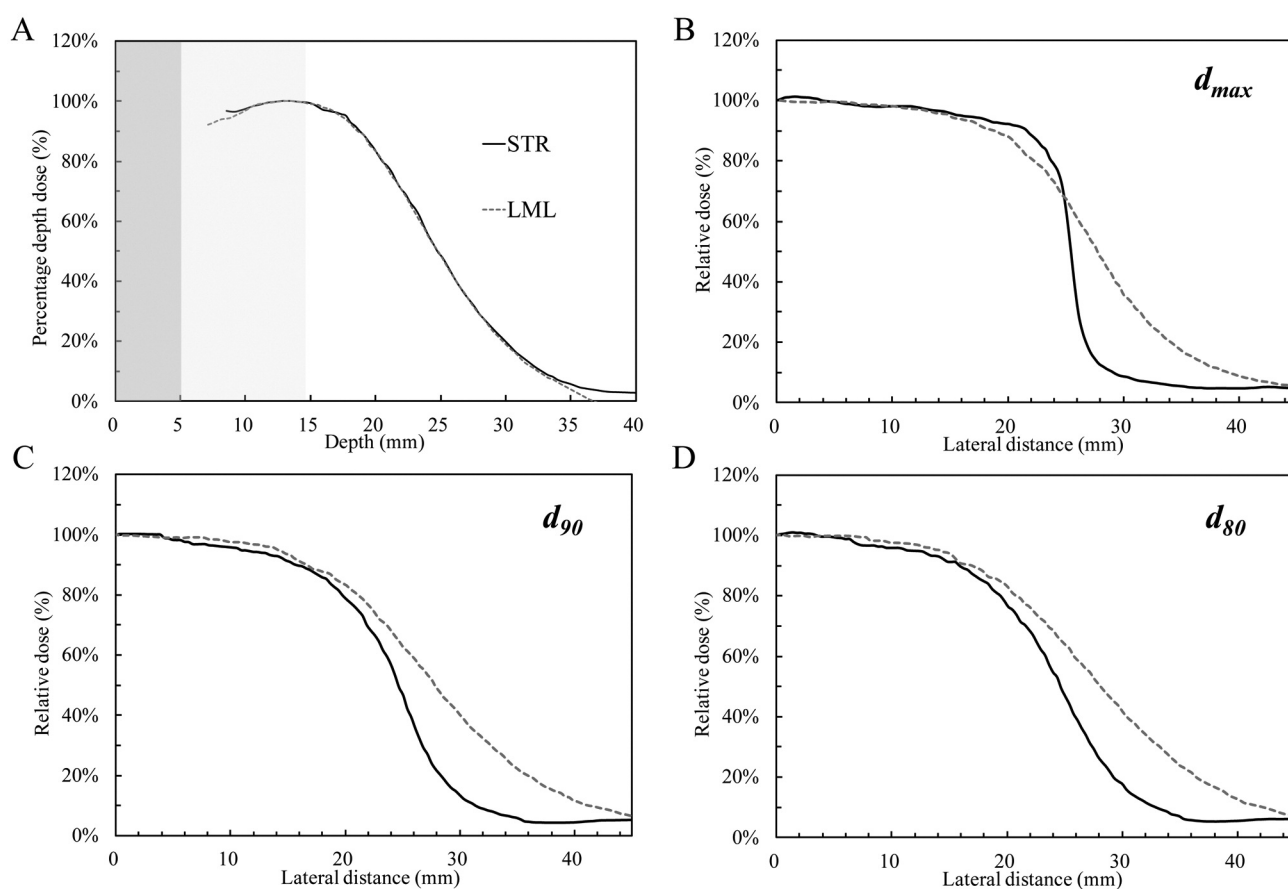


Figure 4. First dosimetric evaluation percentage depth doses (A) and lateral dose profiles on the long axis at maximum dose (d_{max}) (B), 90% dose (d_{90}) (C), and 80% dose (d_{80}) (D) employing the basic variable-shape tungsten rubber.

Results

The 2D dose distributions on the long axis for the first and second dosimetric evaluations are shown in Figure 3. The penumbra for the STR was sharper than that for the LML. No high-dose regions were observed in the region close to the surface of the bolus.

PDDs and lateral dose profiles at d_{max} , d_{90} , and d_{80} on the long axis normalized to the dose at CAX for the first dosimetric evaluation are shown in Figure 4, and the dosimetric characteristics for both evaluations are summarized in Table I. The difference of PDD characteristics between the STR and LML was within 0.4 mm in both dosimetric evaluations. Additionally, the difference between the first and second dosimetric evaluations was within 0.6 mm at each depth. In particular, the difference of the d_{max} between basic and clinical STRs that determine the output factor was 0.6 mm. For the lateral dose profiles, the penumbral widths on long axes for both evaluations are summarized in Table II. The dose increase seen at the irradiation edge in our previous study (22) was not observed, and the maximum dose was approximately 101% at d_{15mm} . The width of the penumbra for the STR was smaller than that for the LML at all depths. Maximum differences of the P_{80-20} were 75.8% and 82.9% in the first and second evaluation, and the differences decreased as the depth increased.

The output factor for the clinical STR was 0.995 and the linac output was 502.6 MU, whereas the output factor for the basic STR was 0.973 and the linac output was 513.7 MU. The total time required for the process of shaping, output factor evaluation, and actual irradiation was reduced from 210 min with LML to 45 min with STR (Table III).

Discussion

In this study, TREAT was applied for keloid scar for the first time worldwide, and the process from shaping of the STR to the delivery was performed successfully. TREAT was completed within 1 hour from shaping to delivery although prior dosimetric evaluation was carried out, which indicates electron radiotherapy might be possible within 1 hour of excision. The depth dose profiles between the basic and clinical STRs were practically similar because the basic STR aperture size was shaped to be close to that of the clinical STR. Thus, the output factor can be easily and immediately evaluated in an actual clinical situation. The patient who underwent the electron radiotherapy with STR has not experienced acute toxicity such as radiodermatitis and no local recurrence has occurred for 1 year.

STR can be shaped by hand at a temperature of approximately 60°C and the STR collimator shape is maintained at room and body temperatures (22). STR can be fit to the rounded contour of a part of a patient's anatomy, such as the face, ear, shoulder, and abdomen easily because

Table I. Dosimetric characteristics of percentage depth dose with variable-shape tungsten rubber (STR) and low-melting-point lead (LML) for the first and second dosimetric evaluations.

Evaluation		Depth (mm)			
		d_{max}	d_{90}	d_{80}	d_{50}
First	STR	12.8	18.4	20.1	24.4
	LML	13.2	18.2	20.0	24.3
Second	STR	13.4	18.2	20.1	24.3
	LML	13.1	18.4	20.2	24.7

d_{max} : Maximum dose; $d_{90/80/50}$: 90%/80%/50% dose.

Table II. Penumbral widths of the lateral dose profiles with variable-shape tungsten rubber (STR) and low-melting-point lead (LML) for the first and second dosimetric evaluations.

Evaluation		Penumbral size (P_{80-20}) (mm)			
		d_{max}	d_{15mm}	d_{90}	d_{80}
First	STR	2.8	4.6	8.1	9.5
	LML	11.6	12.7	14.5	15.2
	Decrease (%)	75.8	63.9	43.9	37.2
Second	STR	2.1	3.5	8.1	10.6
	LML	12.4	14.5	15.9	16.2
	Decrease (%)	82.9	75.6	48.9	34.8

d_{max} : Maximum dose; d_{15mm} : dose under STR/LML; $d_{90/80/50}$: 90%/80% dose.

Table III. Time required from shaping to delivery in electron radiotherapy using variable-shape tungsten rubber (STR) and low-melting-point lead (LML).

		Time (min)		
		Shaping	Output factor evaluation	Delivery
STR	15	15	15	45
LML	180	15	15	210

of its pliability. In this case, the STR can also fit the shape of parts of the auricle, which has irregularities. STR can be also applied as skin field collimation because of its nontoxicity, in stark contrast to LML (22). As previously reported, the dosimetric characters of TFP and TCR are similar to STR (8, 11-21). However, TFP and TCR are not flexible in processing and shaping, therefore, they cannot be fit to body parts with a rounded contour or many bumps like STR can.

The conventional LML collimator away from the body surface caused the wide penumbra shown in Figures 3 and 4. The bolus can enhance the wide penumbra and cause an air gap between the bolus and the surface, resulting in increased dosimetric uncertainty (3, 9, 10, 30-35). In addition, the small irradiation field, in particular, does not establish a lateral electron equilibrium, resulting in a reduced dose (9, 10). Therefore, a large margin is needed for electron radiotherapy with conventional LML and bolus to cover the therapeutic region by the high-dose region (9, 10, 30, 31, 33-35). Conversely, the STR can be set as a skin field collimation due to its nontoxicity; hence, small penumbral widths can be achieved, requiring a much reduced margin than that of the conventional LML collimator whilst maintaining the same PDD characteristics as shown in Figure 4 and Table I. We considered the high-dose spot at the edge of STR to be due to the scatter radiation from the STR in a previous study (22); however, no high-dose area was observed, as shown in Figures 3 and 4 for the geometry with the bolus filling the aperture (simulated the auricle) of the STR. Therefore, significant skin reaction would not occur in this clinical situation.

Antoni *et al.* reported the usefulness of electron radiotherapy with a spoiler made of aluminum for auricular keloid (36). However, this process is labor-intensive and time-consuming, while the STR-shaping process is extremely manageable. STR can be used in electron adaptive therapy (*i.e.* TREAT) for the individualization of treatment for each patient immediately.

Conclusion

The novel method, TREAT, reduced the process time from shaping the irradiation field to delivery and greatly reduced the margin as compared to the conventional LML method. This first clinical experience found the STR to be suitable for use in individualized and immediate electron radiotherapy.

Conflicts of Interest

Hajime Monzen received a research donation from Hayakawa Rubber Co., Ltd. The other Authors declare no competing interests.

Authors' Contributions

Concept and design: YK, MA, TK. Measurements: YK, MA. Data analysis: YK, MT, HM. Treatment: YK, MA. Follow up of the patient: TK. Manuscript preparation: YK, MT, HM. All Authors read and approved the final manuscript.

Acknowledgements

This work was supported by the Japan Society for the Promotion of Science KAKENHI (grant number: 19K08211, 19K17213). We also thank Enago (www.enago.jp) for the English language review.

References

- Giarratano JC, Duerkes RJ and Almond PR: Lead shielding thickness for dose reduction of 7- to 28-MeV electrons. *Med Phys* 2(6): 336-337, 1975. PMID: 811969. DOI: 10.1118/1.594205
- Khan FM, Moore VC and Levitt SH: Field shaping in electron beam therapy. *Br J Radiol* 49(586): 883-886, 1976. PMID: 824008. DOI: 10.1259/0007-1285-49-586-883
- Khan FM, Werner BL and Deibel Jr FC: Lead shielding for electrons. *Med Phys* 8(5): 712-713, 1981. PMID: 7290024. DOI: 10.1118/1.594841
- Prasad SG, Parthasaradhi K, Lee Y and Garces R: Lead shielding thickness for dose reduction of 5 MeV electrons. *Med Phys* 16(5): 807-808, 1989. PMID: 2509872. DOI: 10.1118/1.596432
- Rempel D: The lead-exposed worker. *JAMA* 262(4): 532-534, 1989. DOI: 10.1001/jama.1989.03430040104034
- Needleman H: Lead poisoning. *Annu Rev Med* 55: 209-222, 2004. PMID: 14746518. DOI: 10.1146/annurev.med.55.091902.103653
- Rapisarda V, Ledda C, Castaing M, Proietti L and Ferrante M: Potential exposure to carcinogens in low-melting alloys processing. *G Ital Med Del Lav Ergon* 35(2): 73-76, 2013. PMID: 23914599.
- Kijima K, Monzen H, Matsumoto K, Tamura M and Nishimura Y: The shielding ability of novel tungsten rubber against the electron beam for clinical use in radiation therapy. *Anticancer Res* 38(7): 3919-3927, 2018. PMID: 29970513. DOI: 10.21873/anticancer.12677
- Khan FM, Doppke KP, Hogstrom KR, Kutcher GJ, Nath R, Prasad SC, Purdy JA, Rozenfeld M and Werner BL: Clinical electron-beam dosimetry: report of AAPM Radiation Therapy Committee Task Group No. 25. *Med Phys* 18(1): 73-109, 1991. PMID: 1901132. DOI: 10.1118/1.596695
- Gerbi BJ, Antolak JA, Deibel FC, Followill DS, Herman MG, Higgins PD, Huq MS, Mihailidis DN, Yorke ED, Hogstrom KR and Khan FM: Recommendations for clinical electron beam dosimetry: Supplement to the recommendations of Task Group 25. *Med Phys* 36(7): 3239-3279, 2009. PMID: 1901132. DOI: 10.1118/1.3125820
- Fujimoto T, Monzen H, Nakata M, Okada T, Yano S, Takakura T, Kuwahara J, Sasaki M, Higashimura K and Hiraoka M: Dosimetric shield evaluation with tungsten sheet in 4, 6, and 9 MeV electron beams. *Phys Med* 30(7): 838-842, 2014. PMID: 24953537. DOI: 10.1016/j.ejmp.2014.05.009
- Kamomae T, Monzen H, Kawamura M, Okudaira K, Nakaya T, Mukoyama T, Miyake Y, Ishihara Y, Itoh Y and Naganawa S: Dosimetric feasibility of using tungsten-based functional paper for flexible chest wall protectors in intraoperative electron radiotherapy for breast cancer. *Phys Med Biol* 63(1): 015006, 2017. PMID: 29083315. DOI: 10.1088/1361-6560/aa96cf
- Monzen H, Kanno I, Fujimoto T and Hiraoka M: Estimation of the shielding ability of a tungsten functional paper for diagnostic x-rays and gamma rays. *J Appl Clin Med Phys* 18(5): 325-329, 2017. PMID: 28656739. DOI: 10.1002/acm2.12122
- Monzen H, Tamura M, Shimomura K, Onishi Y, Nakayama S, Fujimoto T, Matsumoto K, Hanaoka K and Kamomae T: A novel radiation protection device based on tungsten functional paper for application in interventional radiology. *J Appl Clin Med Phys* 18(3): 215-220, 2017. PMID: 28422397. DOI: 10.1002/acm2.12083
- Tamura M, Monzen H, Kubo K, Hirata M and Nishimura Y: Feasibility of tungsten functional paper in electron grid therapy:

- A Monte Carlo study. *Phys Med Biol* 62(3): 878-889, 2017. PMID: 28072577. DOI: 10.1088/1361-6560/62/3/878
- 16 Inada M, Monzen H, Matsumoto K, Tamura M, Minami T, Nakamatsu K and Nishimura Y: A novel radiation-shielding undergarment using tungsten functional paper for patient with permanent prostate brachytherapy. *J Radiat Res* 59(3): 333-337, 2018. PMID: 29659976. DOI: 10.1093/jrr/rry030
 - 17 Kawai Y, Tamura M, Amano M, Kamomae T and Monzen H: Dosimetric characterization of a novel surface collimator with tungsten functional paper for electron therapy. *Anticancer Res* 39(6): 2839-2843, 2019. PMID: 31177121. DOI: 10.21873/anticancer.13412
 - 18 Kosaka H, Monzen H, Amano M, Tamura M, Hattori S, Kono Y and Nishimura Y: Radiation dose reduction to the eye lens in head CT using tungsten functional paper and organ-based tube current modulation. *Eur J Radiol* 124: 108814, 2020. PMID: 31945674. DOI: 10.1016/j.ejrad.2020.108814
 - 19 Kijima K, Krisanachinda A, Tamura M, Monzen H and Nishimura Y: Reduction of occupational exposure using a novel tungsten-containing rubber shield in interventional radiology. *Health Phys* 118(6): 609-614, 2020. PMID: 31855596. DOI: 10.1097/HP.0000000000001177
 - 20 Kijima K, Krisanachinda A, Tamura M, Nishimura Y and Monzen H: Feasibility of a tungsten rubber grid collimator for electron grid therapy. *Anticancer Res* 39(6): 2799-2804, 2019. PMID: 31177116. DOI: 10.21873/anticancer.13407
 - 21 Kosaka H, Monzen H, Matsumoto K, Tamura M and Nishimura Y: Reduction of operator hand exposure in interventional radiology with a novel finger sack using tungsten-containing rubber. *Health Phys* 116(5): 625-630, 2019. PMID: 30688684. DOI: 10.1097/HP.0000000000000992
 - 22 Monzen H, Tamura M, Kijima K, Otsuka M, Matsumoto K, Wakabayashi K, Choi MG, Yoon DK, Doi H, Akiyama H and Nishimura Y: Estimation of radiation shielding ability in electron therapy and brachytherapy with real-time variable-shape tungsten rubber. *Phys Med* 66: 29-35, 2019. PMID: 31550531. DOI: 10.1016/j.ejmp.2019.09.233
 - 23 Matsumoto K, Tamura M, Otsuka M, Wakabayashi K, Kijima K and Monzen H: Dosimetric characteristics of a real time shapeable tungsten containing rubber with electron beams. *Nihon Hoshasen Gijutsu Gakkai Zasshi* 76(12): 1248-1255, 2020. PMID: 33342943. DOI: 10.6009/jirt.2020_JSRT_76.12.1248.
 - 24 Wakabayashi K, Monzen H, Tamura M, Matsumoto M, Takei Y and Nishimura Y: Dosimetric evaluation of skin collimation with tungsten rubber for electron radiotherapy: A Monte Carlo study. *J Appl Clin Med Phys*, Accepted.
 - 25 van Leeuwen MC, Stokmans SC, Bulstra AE, Meijer OW, Heymans MW, Ket JC, Ritt MJ, van Leeuwen PA and Niessen FB: Surgical excision with adjuvant irradiation for treatment of keloid scars: A systematic review. *Plast Reconstr Surg Glob Open* 3(7): e440, 2015. PMID: 26301129. DOI: 10.1097/GOX.0000000000000357
 - 26 Cheraghi N, Cognetta Jr A and Goldberg D: Radiation therapy for the adjunctive treatment of surgically excised keloids: A review. *J Clin Aesthet Dermatol* 10(8): 12-15, 2017. PMID: 28979658.
 - 27 Liu CL and Yuan ZY: Retrospective study of immediate postoperative electron radiotherapy for therapy-resistant earlobe keloids. *Arch Dermatol Res* 311(6): 469-475, 2019. PMID: 31041525. DOI: 10.1007/s00403-019-01922-z
 - 28 Petrou IG, Jugun K, Rüegg EM, Zilli T, Modarressi A and Pittet-Cuénod B: Keloid treatment: What about adjuvant radiotherapy? *Clin Cosmet Investig Dermatol* 12: 295-301, 2019. PMID: 31190938. DOI: 10.2147/CCID.S202884
 - 29 Kamomae T, Oita M, Hayashi N, Sasaki M, Aoyama H, Oguchi H, Kawamura M, Monzen H, Itoh Y and Naganawa S: Characterization of stochastic noise and post-irradiation density growth for reflective-type radiochromic film in therapeutic photon beam dosimetry. *Phys Med* 32:1314-1320, 2016. PMID: 27473441. DOI: 10.1016/j.ejmp.2016.07.091
 - 30 Moyer RF, McElroy WR, O'Brien JE and Chamberlain CC: A surface bolus material for high-energy photon and electron therapy. *Radiology* 146(2): 531-532, 1983. PMID: 6401364. DOI: 10.1148/radiology.146.2.6401364
 - 31 Sharma SC and Johnson MW: Surface dose perturbation due to air gap between patient and bolus for electron beams. *Med Phys* 20(2): 377-378, 1993. PMID: 8497226. DOI: 10.1118/1.597079
 - 32 Perkins GH, McNeese MD, Antolak JA, Buchholz TA, Strom EA and Hogstrom KR: A custom three-dimensional electron bolus technique for optimization of postmastectomy irradiation. *Int J Radiat Oncol Biol Phys* 51(4): 1142-1151, 2001. PMID: 11704339. DOI: 10.1016/s0360-3016(01)01744-8
 - 33 Kong M and Holloway L: An investigation of central axis depth dose distribution perturbation due to an air gap between patient and bolus for electron beams. *Australas Phys Eng Sci Med* 30(2): 111-119, 2007. PMID: 17682400. DOI: 10.1007/bf03178415
 - 34 Khan Y, Villarreal-Barajas JE, Udowicz M, Sinha R, Muhammad W, Abbasi AN and Hussain A: Clinical and dosimetric implications of air gaps between bolus and skin surface during radiation therapy. *J Cancer Ther* 4(7): 1251-1255, 2013. DOI: 10.4236/jct.2013.47147
 - 35 Mahdavi H, Jabbari K and Roayaei M: Evaluation of various boluses in dose distribution for electron therapy of the chest wall with an inward defect. *J Med Phys* 41(1): 38-44, 2016. PMID: 27051169. DOI: 10.4103/0971-6203.177288
 - 36 Capel AV, Palop JV, Olivé AP and Fernándezc ASR: Adviance in refractory keloids using electron beams with a spoiler: Recent results. *Rep Pract Oncol Radiother* 20(1): 43-49, 2015. PMID: 25535584. DOI: 10.1016/j.rpor.2014.08.005

Received December 7, 2020

Revised December 18, 2020

Accepted January 4, 2021